THE ASTROPHYSICAL JOURNAL, 459:307–321, 1996 March 1

ANALYSIS OF THE POLARIZATION AND FLUX SPECTRA OF SN 1993J

P. HÖFLICH
Center for Astrophysics, Harvard University, Cambridge, MA 02138; pah@cfa141.harvard.edu
J. C. WHEELER
Department of Astronomy, University of Texas, Austin, TX 78712; wheel@astro.as.utexas.edu
D. C. HINES
Steward Observatory, 933 North Cherry Avenue, Tucson, AZ 85721; dhines@neutrino.physics.arizona.edu
AND
S. R. TRAMMELL
The Enrico Fermi Institute, The University of Chicago, 5640 South Ellis Avenue, Chicago, IL 60637; srt@oddjob.uchicago.edu
Received 1995 April 6; accepted 1995 September 1

ABSTRACT

Synthetic polarization and flux spectra are presented for aspherical, electron scattering–dominated photospheres of Type II supernovae (SN II's) in general and the specific case of SN 1993J. Monte Carlo calculations are based on the following assumptions: (1) ellipsoidal envelopes with power-law density profiles; (2) occupation numbers given by local thermodynamical equilibrium (LTE); (3) pure electron scattering for continuum opacities; (4) lines treated in a Sobolev approximation with an assumed constant thermalization fraction; (5) line transitions result in depolarization; and (6) the temperature structure is given by a gray extended atmosphere.

The observed luminosity of a Type II supernova depends on the unknown inclination angle *i*. Spectral analysis alone will fail to detect even strong deviations from spherical symmetry. Line scattering depolarizes incident polarized light, but the residual intrinsic polarization does not completely vanish because of electron scattering effects that depend on the electron density distribution. By combining results on the polarization and velocity structure of the emission lines and the degree of polarization in the continuum, we place strong constraints on the degree of asphericity, the inclination of the system, and the electron density distribution. In addition, since the problem is overconstrained, we can independently test for the contribution to the polarization caused by aligned interstellar grains between the supernova and Earth.

These modeling techniques have been applied to SN 1993J. Both the flux spectra and the percentage of polarization as a function of wavelength can be reproduced by an aspherical model with an axis ratio of 0.6, radial electron densities proportional to r^{-5}, and an effective temperature of 4800 K. In an oblate model, SN 1993J is seen almost equator-on. The line-forming region is still within the hydrogen-rich part of the envelope 3 weeks after the explosion, although the continuum may form in deeper layers. Although the residual polarization across Hα is not zero, the interstellar component derived herein is consistent with that deduced and reported by Trammell et al. in 1993. The power of this technique for investigating the structure of other SN II's, as a method for independently deriving the interstellar polarization, and the implications of these results on the use of SN II's to determine distances through the Baade-Wesselink method are discussed.

Subject headings: polarization — radiative transfer — supernovae: general — supernovae: individual (SN 1993J)

1. INTRODUCTION

The investigation of the emitted light of Type II supernovae (SN II's) is important for various fields in astronomy and astrophysics. The observed spectra, spectropolarimetry, and light curves give direct information on the physical, geometrical, and chemical conditions of the expanding envelope. In principle, this allows us to test dynamic models of the ejecta from supernovae and to investigate the explosion mechanism of SN II's and the final stages of the evolution of massive stars. Because SN II's are among the brightest single objects, they are also commonly used as distance indicators based on the Baade-Wesselink method (Baade 1926; Wesselink 1946; Höflich, Wehrse, & Shaviv 1986; Höflich 1988, 1991a; Eastman & Kirshner 1989; Baron, Hauschildt, & Branch 1994; Schmidt et al. 1994), but this method depends critically on the assumption of spherical envelopes. Little attention has been paid, however, to polarization measurements that are crucial to test this assumption and investigate the overall geometry.

Very few polarization measurements are available for supernovae. SN 1968L (Serkowski 1970) and SN 1970G (Shakhovskoi & Efimov 1973) were Type II supernovae. SN 1968L was not isolated from the ISM, but SN 1970G was probably intrinsically polarized at the level of 0.5%–1%. Three Type Ia events have been reported with no detectable polarization above the interstellar component: SN 1972E (Wolstencraft & Kemp 1972), SN 1983G (McCall et al. 1984; McCall 1985), and SN 1992A (Spyromilio & Bailey 1993). One Type Ib supernova, SN 1983N, known to have a significant circumstellar nebula, has been detected (McCall et al. 1984; McCall 1985). Several recent events have also been observed: SN 1994D, SN 1994ae, and SN 1995, Type Ia with low polarization; SN 1994Y, a narrow-line Type II that shows polarization at the level of 1.5%–2%; and

SN 1995H, another Type II with detectable polarization at about the 1% level (Wang et al. 1996).

The best polarization data to date are for SN 1987A and SN 1993J. For SN 1987A, polarization of up to 0.5% was observed early on but decreased rapidly over the next few weeks (Méndez et al. 1988; Clocchiatti et al. 1988; Cropper et al. 1987). It was concluded that the envelope of SN 1987A showed asphericities of about 10%–20% and that Thomson scattering was the main physical effect causing the polarization (e.g., Méndez et al. 1988; Höflich 1991a; Jeffery 1991). Whether the asymmetry implied by the polarization measurements is caused by rapid rotation of the progenitor (Höflich & Steinmetz 1991; Steinmetz & Höflich 1992) or by an asphericity of the SN II explosion mechanism itself (Yamada & Sato 1991) is still a question under debate. Depending on the answer, asphericity, and thus observable polarization, may prove to be a common property of SN II's or may just be related to the special nature of SN 1987A (Arnett et al. 1989; Hillebrandt & Höflich 1990). If it is common, then it may significantly impact the use of supernovae to estimate distances (McCall 1985).

SN 1993J was observed from the beginning in wavelength bands from X-ray to radio. Soon after the discovery, the spectral evolution and the light curves made it clear that SN 1993J—like SN 1987A—did not represent a typical SN II. Although details related to the progenitor evolution and the relation between initial mass and He/C-core mass are disputed, general agreement was soon achieved that SN 1993J represents an object that had lost most of its H-rich envelope prior to the explosion with a remaining H-rich mass of ≈ 0.2–$1.5\ M_\odot$ (Höflich, Langer, & Duschinger 1993; Wheeler et al. 1993; Swartz et al. 1993; Woosley et al. 1994; Shigeyama et al. 1994; Jeffery et al. 1994). The progenitor was a red or yellow supergiant that underwent very strong mass loss, as confirmed by observations in the radio and X-ray (Van Dyk et al. 1994; Fransson, Lundqvist, & Chevalier 1996). For reviews see Wheeler & Filippenko (1995) and Baron, Hauschildt, & Young (1995)?

Unlike SN 1987A, the polarization was already high ($\gtrsim 1\%$) in SN 1993J only a few days after the onset of explosion and increased to $\approx 1.6\%$ 3 weeks later (see § 4). A strongly differential stellar rotation, as suggested for SN 1987A, can be ruled out because the progenitor of SN 1993J had an extended and hence presumably slowly rotating envelope. Höflich (1994) studied different configurations that may explain the polarization in the continuum. From the size of the polarization and its weak dependence on time, Höflich concluded that an aspherical explosion is unlikely. Neither mechanism suggested for SN 1987A is thus easily applicable in this case. Höflich found that the polarization can be explained by an oblate ellipsoid with axis ratio of 0.6 or by "off-center" sources that may have been caused by the explosion in a very close binary system or by a strong "kick" of the neutron star during the explosion. In principle, these scenarios can be distinguished by the time evolution of the polarization, but a lack of observations has prevented clarification. A critical point is that the value of 0.6 for the asphericity is a lower limit, valid only if SN 1993J is seen from the equatorial plane. Höflich's analysis relied on the correction of the measured total polarization for the interstellar component (Trammell, Hines, & Wheeler 1993). As the polarization is a (pseudo)vector, the size and temporal behavior of the intrinsic component of the polarization depend sensitively on the correction for the interstellar component. An independent check of the value of the ISM polarization derived by Trammell et al. (1993) is appropriate.

Asphericity may be a common phenomenon in SN II's since it has been observed in both cases that have been sufficiently bright to allow for polarization measurements. In this paper we will study asphericity effects both on the total flux spectra and the percent polarization as a function of wavelength. In this paper these will be referred to as the *flux spectra* and *polarization spectra*, respectively. Note that the percent polarization is to be distinguished from the Stokes flux spectrum as constructed and presented in Trammell et al. (their Fig. 2; see also § 4). The following questions will be addressed: Does the wavelength dependence of the polarization provide additional information on the envelope structure? Can we determine the inclination i at which a supernovae is observed? Can the interstellar component be determined independently? Do the flux spectra constrain possible asphericity effects? and can we infer from successful fits of SN II spectra with spherical models that the envelopes are indeed spherical, as suggested by Baron et al. (1994)?

The underlying physical model is described in § 2. General results of our calculations are discussed in the following section. Polarimetric observations of SN 1993J are summarized in § 4, and a comparison of the current model with observations is given in § 5. Implications for the density and chemical structure of SN 1993J are discussed. Consistency checks between flux and polarization spectra are performed to test the interstellar polarization correction applied by Trammell et al. (1993). Our conclusions are presented in § 6.

2. COMPUTATIONAL METHOD

The current calculations use a modified version of the Monte Carlo code previously applied to calculate the continuum polarization in SN 1987A and SN 1993J (Höflich 1988, 1991, 1995). The code is capable of handling arbitrary three-dimensional geometries, both for the density and the distribution of the sources. Polarization and flux spectra for rapidly expanding envelopes can thus be computed.

Little is known about the shape of the envelopes in SN II's in general and SN 1993J in particular. Therefore, we use oblate ellipsoids parameterized by

$$x^2 + y^2 + z^2/E^2 = r^2 , \qquad (1)$$

where x, y, and z are orthonormal directions, E is the axis ratio of a rotational ellipsoid, and $r \epsilon [A_{\rm min}, A_{\rm max}]$. $A_{\rm min,max}$ are the minimum and maximum distances in the equatorial plane of the inner and outer boundaries, respectively.

The inner boundary is at $\tau_{\rm sc} = 3$ (the approximate thermalization depth, see below). Höflich (1994) found that the continuum polarization observed for SN 1993J can be understood in terms of ellipsoids. In the following $E = 0.6$ is used as a canonical value.

Shortly (hours to a few days) after the core collapse, the expansion of the shell becomes homologous, i.e., the velocity becomes proportional to the distance from the center. Piecewise, the density slope can be approximated by power laws, i.e., $\rho \propto r^{-n}$. The ratio of density scale height to radius is thus $1/n$.

For computations of polarization and flux spectra, line blocking is included in the Sobolev approximation (Sobolev

1957). The implementation is similar to that described by Abbot & Lucy (1985) for their one-dimensional Monte Carlo code.

It is well known that deviations from local thermodynamical equilibrium are important if details of individual lines are to be understood (see, e.g., Lucy 1988; Höflich 1988; Eastman & Kirshner 1989; Baron et al. 1994). Detailed NLTE calculations consistent with three-dimensional radiation transport including polarization are beyond the capabilities of available computers. On the other hand, at least qualitative agreement with the observations can be achieved if LTE population numbers are assumed (Branch et al. 1981; Harkness 1991; Jeffery et al. 1994; Wheeler et al. 1994). Several simplifications are thus adopted similar to those applied in the framework of spectral modeling in one-dimensional calculations. The population numbers are assumed to be in local thermodynamic equilibrium. For He, the importance of nonthermal excitation by gamma rays is well established (Swartz et al. 1993). This effect is mimicked here by an artificial enhancement of the He opacity (see discussion in § 5).

Thomson scattering is assumed to be the only source of opacity in the continuum. Lines are treated in a scattering approximation with the thermalization fraction ϵ of 10^{-2}. This value is based on detailed NLTE calculations (Höflich 1995). If a photon is absorbed in a line, it will be reemitted at the same frequency (in the comoving frame) with a probability of $(1 - \epsilon)$ or it will be thermalized, i.e., reemitted at a frequency randomly chosen according to the local blackbody function. In general, complete redistribution can be assumed for the line profiles (Mihalas 1978) since collisional processes dominate the relative level populations within the fine structure of the upper and lower atomic level of a line transition. Timescales for collisional redistribution are much shorter than absorption and reemission processes in a line. Since collisions are random processes, all information on nonlocal processes (i.e., polarization) is lost. Therefore, we can assume that a photon becomes unpolarized if absorbed and reemitted in a line.

The temperature structure $T(r)$ is given by an extended gray atmosphere calculation, which gives a good approximation to NLTE atmospheres (Eastman & Kirchner 1989; Höflich 1989, 1990, 1991b). At small optical depths ($\tau \leq 0.3$) the excitation temperature is taken to be constant since the lines are mainly scattering dominated.

The thermalization optical depth of continuum photons is about 3–5 Thomson scattering optical depths (e.g. Hershkowitz, Lindner, & Wagoner 1986; Höflich et al. 1986), where τ is measured in the radial direction. The light becomes unpolarized at large optical depths, both by thermalization and multiple scattering processes. The inner boundary condition is given by isotropic emission at the thermalization depth τ_{max}. Photons are absorbed and reemitted if they propagate to the inner boundary during their random walk. In contrast to the optically thin case (Brown & McLean 1977), the polarization depends only slightly on τ_{max} for $\tau_{max} \gtrsim 2$ (Daniel 1982; Höflich 1991). Thus, we use $\tau_{max} = 3$ as our standard value. Accordingly, at this inner boundary, the radiation field is assumed to be given by a local blackbody.

The optical depth is closely related to the question of the photospheric radius, which is often used as a basic parameter to characterize the atmospheres of supernovae. This radius is that which would be observed in the spectral continuum if the object were resolved in angle. It may be defined by the radial distance R_{true}, where the optical depth in true absorption becomes unity; R_{therm}, where the photons thermalize (i.e., the radius at which most of the emitted photons are formed); or R_{sc}, where the photons most likely undergo electron scattering before escape. In addition, the photospheric radius is a function of frequency and that function will vary with the definition of opacity, namely whether monochromatic, broadband, Rosseland, or Planck means are used. For a more detailed discussion see, e.g., Höflich (1987, 1990, 1995) or Baschek, Scholz, & Wehrse (1991), where it has been shown that the Doppler shift of the absorption of weak lines provides a good measurement of the last scattering radius. For nonspherical geometries, the situation is even more complicated since the radial direction is not orthogonal to the shells of constant density. For any definition, R_{ph} becomes a function of the inclination angle i of the line of sight with respect to the direction along which the optical depth is measured. The latter is aligned with the density gradient, the direction of the highest escape probability for photons, and is taken to be the radial direction in the current work. Thus, R_{ph} does not have an exact physical meaning but may be used for convenience to provide some guidance to imagine the physical situation. Here, R_{ph} is defined as the radial distance in the equatorial direction and we set $R_{ph} = R_{sc}$ since we are dealing with the interpretation of normalized spectra and R_{sc} can be measured approximately by the Doppler shift of weak lines.

In conclusion, we use the following assumptions: (1) ellipsoidal (oblate) geometry (eq. [1]); (2) power-law density profiles; (3) velocity $v \propto r$; (4) LTE occupation numbers except for He; (5) pure scattering approximation for the continuum and scattering lines with a thermalization fraction of 10^{-2}; (6) depolarization in lines; and (7) $T(r)$ given by the gray extended atmosphere for the optically thick layers and T being constant in the outer, optically thin layers. The free parameters are (1) photospheric radius R_{ph}, (2) effective temperature T_{eff}, (3) density exponent n, (4) axis ratio E, and (5) enhancement factor for helium opacities.

In the actual calculations, the angular space of the emitted photons is discretized by 20 bins in the inclination angle i defined to be zero on the symmetry axis. The spectral resolution is $\Delta\lambda/\lambda \approx 150$. The calculations are halted when the residual error in the percentage polarization P becomes less than 0.1% (i.e., $P = 1.6\% \pm 0.1\%$).

3. THE CALCULATIONS

The large parameter space makes impractical a presentation of a grid of models covering SN II's in general. Instead, we have studied models applicable to SN 1993J at about 23 days past explosion. We chose oblate ellipsoids with an axis ratio E of 0.6 and consider power-law density profiles with exponents between -3 and -7 because those are expected for the envelope of SN 1993J independent of the progenitor mass or model (Höflich et al. 1993; Shigeyama et al. 1994; Woosley et al. 1994). Effective temperatures and the photospheric velocities range between 4500 and 5500 K and 4500 and 5500 km s^{-1}, respectively. The photospheric radius R_{ph} follows directly from v_{ph} and the time of observation. In practice, we have adjusted the photospheric density ρ_{ph} to produce R_{ph}. We assume an equal amount of hydrogen and helium, a solar mixture of heavier elements, and for simplicity we ignore composition gradients. The latter assumption will be discussed in the conclusions. Table

TABLE 1

MODEL PARAMETERS

Model	$T_{\rm eff}$ (K)	$v_{\rm ph}$ (km s^{-1})	$\rho_{\rm ph}$ (g cm^{-3})	n	E
H3cHe	4800	6600.	6.55E−13	3	0.6
H5cHe	4800	6600.	2.25E−12	5	0.6
H7cHe	4800	6600.	4.35E−12	7	0.6
H3sphere.....	4800	5280.	8.20	3	1.0

1 gives the parameters and some related quantities for those models that we discuss in detail.

Deviations from sphericity will result in a directional dependence of the computed luminosity, i.e., $L = L(i)$. Consequently, the total luminosity cannot be deduced from observations without taking the asphericity into account. This may have strong implications for the interpretation of light curves and the use of SN II's as distance indicators (Höflich 1991a, 1994). This effect is illustrated in Figure 1 for the current models. The small differences in $L(i)$ between the models with different density profiles can be understood in terms of multiple scattering of the continuum which decreases with increasing density gradients. The variation of luminosity with inclination will be a strong function of the ellipticity, E. Although these models do not have a fully self-consistent temperature structure, we believe this effect of inclination on luminosity to be general.

The general properties of our model spectra can be discussed in terms of representative models. We first consider models with $T_{\rm eff} = 4800$ K, $v_{\rm ph} = 5500$ km s^{-1}, $R_{\rm ph} = 10^{15}$ cm and power-law density gradients with n of 3 (H3cHe) and 5 (H5cHe). All flux spectra presented in the figures have been normalized to the flux at 7000 Å for convenience of presentation.

Before discussing the overall spectra, the region of Hα is studied because the opacities are dominated by Thomson scattering and only a single line (assuming He I λ6678 to be negligible at this epoch). In Figure 2, the emitted flux and polarization spectra are given for inclination angles of 90°, 65°, and 30°, that is from looking directly along the equator to nearly down the symmetry axis.

The line fluxes can be generally understood by analogy with spherical envelopes. The density gradient determines the extension of the line-forming region. For homologous expansion, position translates into frequency or wavelength space. Both the absorption and emission components become smaller with larger density gradients. For optically thick lines, the absorption minima occur at expansion velocities in excess of the photospheric velocity $v_{\rm ph}$ because they are formed well above the photosphere. Thus, lines of different optical depth allow for a test of density gradients. For a more detailed discussion of these and related questions, see Höflich (1990, 1991a) and Duschinger et al. (1994).

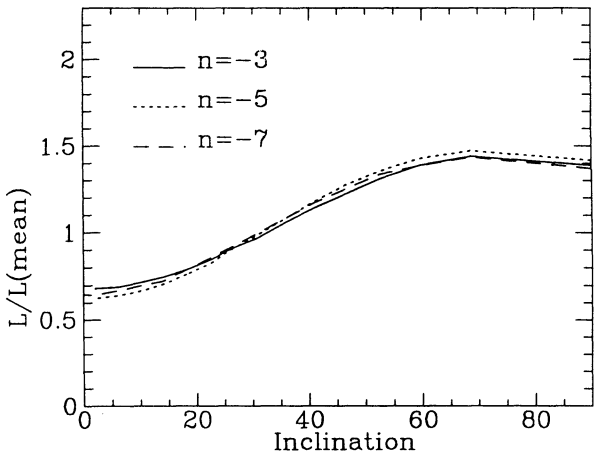

FIG. 1.—Frequency mean of the luminosity as a function of the inclination angle for the models given in Table 1.

The main effect of asphericity is a change of the Doppler shifts in lines with the inclination i (Fig. 2). The absorption component becomes sharper and less blueshifted if observed from lower inclinations (i.e., more pole-on). For both H3cHe and H5cHe, the ratios between the Doppler shifts at $i = 90°$ to that at $i = 30°$ for both the absorption minima and blue edges are in the range 0.75–0.8. This is consistent with the corresponding ratios of the radial distance of the photosphere $R_{\rm ph}(i)$.

We can construct a corresponding spherical model if we set the photospheric radius for the spherical model equal to that for the ellipsoidal model along a given line of sight, i.e., $R_{\rm ph} = R_{\rm ph}(i)$ (Fig. 3). Even better agreement can be achieved if we would allow for an artificial adjustment of the intrinsic line width by introducing a "microturbulence" (Höflich 1988). We conclude that although the emitted flux is very dependent on the inclination, observations of the flux spectra alone are not sufficient to distinguish spherical and nonspherical geometries.

Now, consider the polarization P_λ (Fig. 2). In the illustrated examples, F_λ changes by only 50% over the Hα feature, whereas P_λ varies by a factor of 3–10 depending on the inclination. In general, the continuum polarization increases if the object is observed more directly on the equator (i.e., from large inclinations i). The polarization does not increase as $\sin^2(i)$ as would be expected for optically thin envelopes. The reason is that the depolarizing effects of multiple scattering cause information on the global geometry to be lost, thus reducing the emergent continuum polarization (Höflich 1991a). Because of the polarizing effects of Thomson scattering, we cannot assume that $P \to 0$ even in the strong Hα line where multiple scattering may be important. This becomes significant in evaluating the effect of the ISM as discussed in § 5.

As for the flux, the polarization profiles become narrower with increasing density gradients. Depolarization of a photon requires only one absorption in a line, whereas several interactions are required to change the flux F_λ and the local source functions by thermalization. Even thermalization has little effect on the absolute flux over a line if, as we assume here, the temperature gradients in the atmosphere are typically small. In addition, the depolarizing effect of multiple scattering is more important for radially extended atmospheres and hence for small density gradients. The result, as illustrated in Figure 2, is that P_λ is much more sensitive to the density profile than is F_λ.

The breadth of the minimum in the polarization spectrum provides additional information on the density gradient that is not available from the flux alone. For steeper density gradients, the particle density is higher at a given Thomson scattering optical depth (see Table 1). For highly ionized gas this implies that the number of neutral particles is also higher at a given optical depth. The Thomson optical depth depends linearly on the density, but the number density of neutral hydrogen formed by recombination is

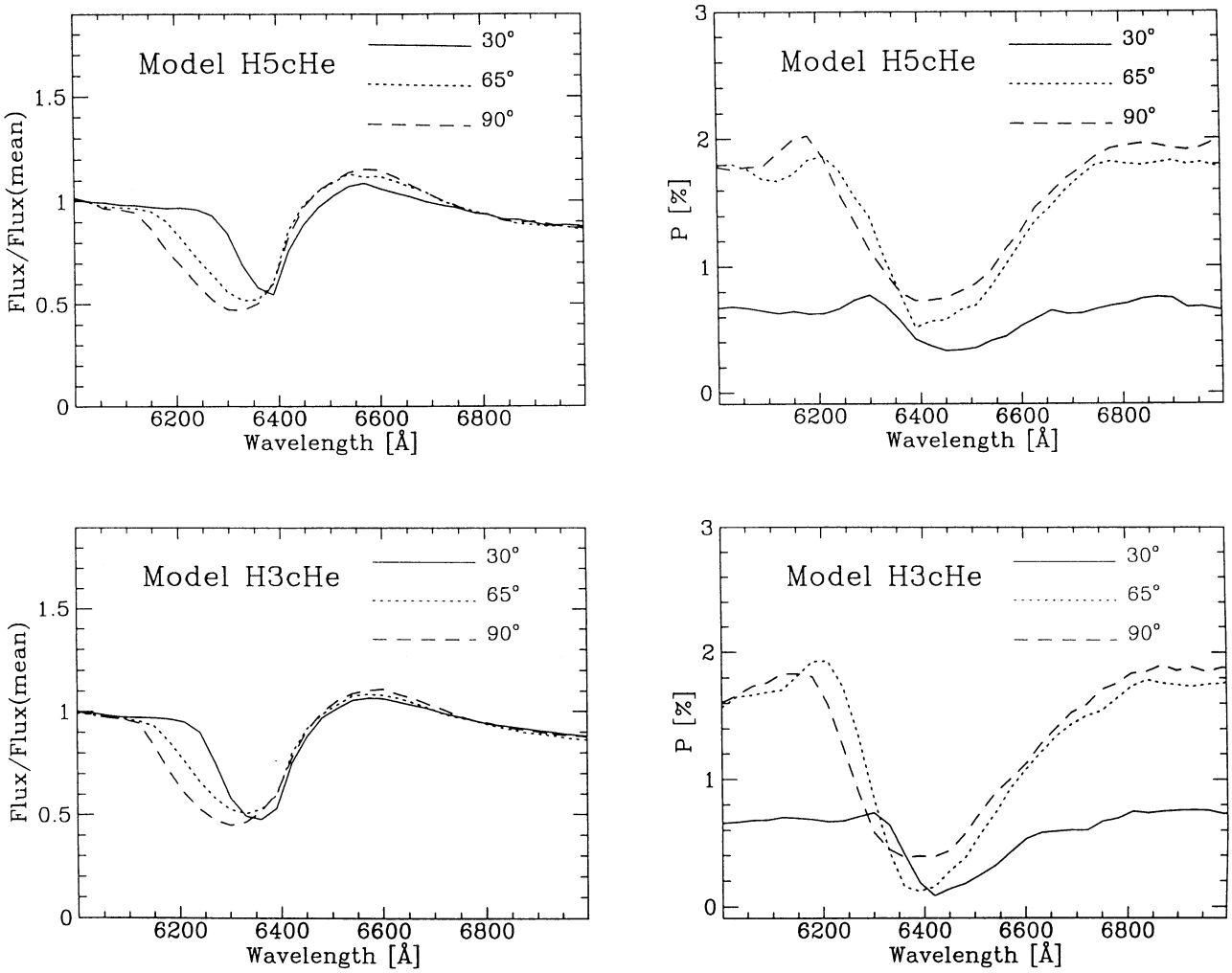

FIG. 2.—Flux and polarization spectra for different inclinations for models with $n = 3$ (*upper graphs*) and $n = 5$ (*lower graphs*). Polarization ($E = 0.6$, $\tau = 3$, $T_{\rm eff} = 4800$ K, $T_c = 6000$ K).

quadratic in the density. The result is that the line absorption of H I will be stronger compared to Thomson scattering in a steeper density gradient. This will result in a stronger depolarization of the lines. If H is mostly ionized, the bottom of the profile in the polarization spectrum becomes slightly broader compared to its total width with increasing density gradient.

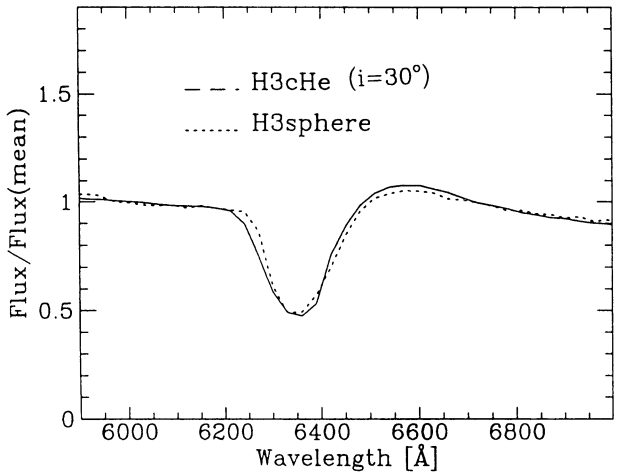

FIG. 3.—Flux of H3cHe seen at an inclination of 30° in comparison to a spherical model with a $R_{\rm ph}$ and $v_{\rm ph}$ being reduced by 20%.

Changing the density gradient alters the flux and polarization spectra in different ways at different wavelengths. This is illustrated in Figure 4. For temperatures larger than 4500–5000 K, line blocking due to singly ionized elements of the iron group increases with increasing density gradient because of the larger particle densities as just described. In the range of $T_{\rm eff}$ under consideration, this effect works mainly at and below the photosphere. In regions governed by a large number of weak lines, the flux is thus mainly determined by layers at large optical depths. On the other hand, polarization is produced in layers of small optical depth since multiple scattering reduces P_λ at large optical depth. The resulting effect can be seen in the spectra of Figure 4 between 4800 and 5500 Å. The flux F_λ of H5cHe is reduced in comparison to H3cHe, whereas P_λ shows little effect. Altering the density gradient alters the fluxes and polarization in a different manner near Hα than in the 5000 Å region. These differences provide a sensitive diagnostic tool.

Line blocking depends sensitively on such factors as $T_{\rm eff}$ and the chemistry. Thus the models presented in this section should not be taken too literally. Nevertheless, these models should qualitatively represent a typical SN II photosphere close to the recombination phase.

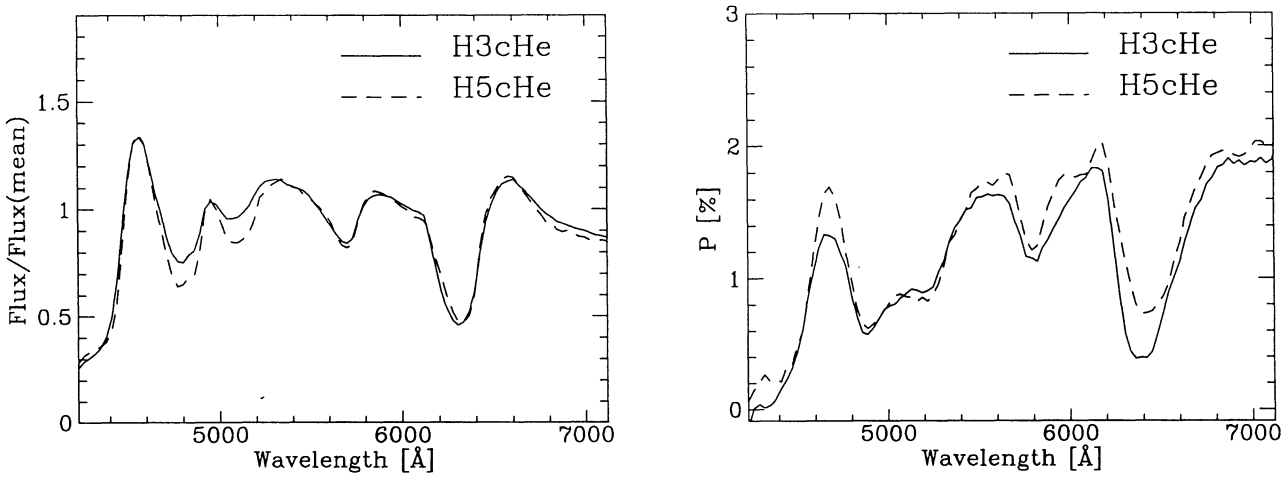

FIG. 4.—Flux and polarization for H3cHe and H5cHe seen at $i = 90°$. Polarization ($E = 0.6, \tau = 3, T_{\rm eff} = 4800$ K, $T_c = 6000$ K).

4. SPECTROPOLARIMETRY OF SN 1993J

SN 1993J was discovered on March 28.9 on the rise to its first maximum. It went through a minimum about April 5 and then a second maximum in V on April 18. Spectropolarimetry was obtained on April 3.2 and 4.2 by Bjorkman & Nordsieck (1993) at the University of Wisconsin Pine Bluff 0.9 m telescope. Weighted over the spectral range 3200–7600 Å, the results were 0.73% ± 0.13% at a position angle of 179°.5 and 0.22% ± 0.16% at a position angle of 41°, respectively. The spread in these data is probably due to effects caused by the nearly full Moon. Formally combining the two data sets gives 0.46% ± 0.1% at a position angle of 5° ± 6°. Measurements made on April 7.22 UT by Smith (1993) yield a V-band polarization of 0.19% ± 0.11% at a position angle of 178° ± 17°. Observations of foreground stars along the direction to SN 1993J showed less than 0.1% polarization, indicating that the observed polarization in SN 1993J is not caused by interstellar polarization within our Galaxy.

Spectropolarimetry was obtained at McDonald Observatory on April 20 (Trammell et al. 1993). The total polarization in the continuum was measured to be 0.9% ± 0.1% at a position angle of 33° ± 3°, nearly independent of wavelength. The percent polarization decreased at the location of Hα, and the position angle rotated by about 10°–15°. On April 26, Jannuzi et al. (1993) measured a polarization of 1.04% at PA = 29° with similar structure at Hα. These results are consistent with those of Trammell et al. (1993) within the errors. The polarization structure across Hα alone proves that SN 1993J was intrinsically polarized and that the lines and continuum had different polarizations regardless of any correction for interstellar polarization.

At Hα the polarized flux consists of the underlying continuum of the supernova and the flux in the emission line, both affected by any polarization induced by the intervening interstellar medium (ISM). After vector subtraction of the continuum polarization, Trammell et al. found the polarization of Hα emission alone to be 1.1% ± 0.1% at a position angle of 150° ± 4°, similar in degree to the observed continuum, but with a significantly different position angle. The orientation of this derived Hα component is compatible with the position angle of the corresponding spiral arm on which SN 1993J is superposed, suggesting that this component could be produced entirely by dust aligned by the magnetic fields that thread this spiral arm. Radio Faraday rotation measurements support this interpretation since they imply that the local magnetic field closely follows the spiral arm containing SN 1993J at a position angle ≈150° (Kraus, Beck, & Hummel 1989). As mentioned above, the local Galactic contribution to this polarization is expected to be minimal. Trammell et al. assumed that Hα was intrinsically unpolarized and that its derived polarization (after vectorially subtracting the continuum) was identical to that induced by the ISM in the spiral arm of M81. They then isolated the intrinsic polarization of the supernova by correcting the total polarized flux for the interstellar contribution by means of a Serkowski law as parameterized by Wilking et al. (1982). The result for the average continuum polarization of the supernova is then 1.6% ± 0.1% at a position angle of 49° ± 3°, both independent of wavelength. The continuum polarization intrinsic to the supernova was thus found to be significantly larger than the total observed continuum polarization (i.e., 1.6% vs. 0.9%). The position angle after correction for the ISM component is essentially independent of wavelength (Trammell et al., Fig. 1). This is evidence that the ISM has been properly isolated and subtracted since it is consistent with the source of the polarization being wavelength-independent electron or dust scattering (Höflich 1991a; Jeffery 1991).

After correction for the interstellar polarization within M81, Trammell et al. isolated the scattered continuum radiation by forming the Stokes flux. This is done by rotating all the polarization into a single, rotated Stokes parameter and then multiplying by the total flux (e.g., Miller & Goodrich 1990). The intrinsic Stokes flux from the supernova computed in this way shows no peak at the rest wavelength of Hα, by construction (i.e., Hα is assumed to be intrinsically unpolarized). The Stokes flux spectrum shows a broad minimum to the blue of Hα of (Trammell et al., Fig. 2). This feature has a minimum at ∼6330 Å corresponding to a velocity of 10,500 km s^{-1} relative to the central wavelength of the emission-line peak, and a FWZI of ∼395 Å corresponding to a velocity range of 18,700 km s^{-1}.

Trammell et al. presented the percent polarization as a function of wavelength for the total contribution but did not present the same quantity, the polarization spectrum as

defined here, corrected for the ISM. These data are presented here (Figs. 6, 7, and 8). The polarization spectrum shows a broad, somewhat asymmetric minimum at about 6500 Å.

Spectropolarimetry data obtained on April 26 at Steward Observatory (Schmidt 1995) and on April 30 by Tran & Filippenko (1993) at Lick Observatory, both with excellent signal-to-noise ratio, confirm the basic interpretation of the spectra given by Trammell et al. The Steward data, and additional Lick observations (Tran & Filippenko 1993; Miller 1993), show a rotation of the position angle across Hα that persists even after the ISP component derived by Trammell et al. has been subtracted. It is difficult to know whether such an effect is revealed by the superior signal to noise ratio or whether it is due to real changes in the polarized flux as the supernova evolves (both data sets were obtained during a period of rapid spectral evolution). This rotation does suggest a small polarization at Hα intrinsic to the supernova. This is possible because, as pointed out in § 3, there can be some residual polarization induced by electron scattering in the line-forming region. The different position angle compared with the continuum would then suggest slightly different scattering geometries for the emission lines and the continuum.

Note that if the ISM component has been correctly isolated by Trammell et al. as 1.1% at a position angle of 150°, then the early measurements of Bjorkman & Nordsieck (1993), and especially the "null" result reported for April 7 by Smith (1993), 0.19% ± 0.11% at a position angle of 178° ± 17°, require special attention.[1] The ISM value cannot change with time. If there is a finite contribution from the ISM, then the supernova must contribute in some way to produce a net null result.

Formal vector subtraction of the ISM polarization deduced by Trammell et al. from the total polarization of the combined data of Bjorkman and Nordsieck and the total measured in V by Smith yields a polarization for the supernova on April 3–4 of 1.0% ± 0.1% at a position angle of 48° ± 6° and on April 7 of 1.0% ± 0.2% at position angle 55° ± 6°. This implies that the supernova already had a polarized component on April 3–4 and on April 7, just before and just after the first minimum, respectively. The data also suggest that the polarization did not change appreciably in either amplitude or orientation at that interesting early phase.

The close similarity of the position angles of the polarized flux intrinsic to the supernova for these two early data sets compared to the corresponding value derived on April 20 by Trammell et al. of 49° ± 3° is remarkable. Note that this angle, ~50°, is significantly different from the position angle of any other component, that is, the ISM. This strongly suggests that the intrinsic polarization from the supernova was roughly constant or perhaps slightly increasing from ~1% on April 3–7 to ~1.6% on April 20 at essentially constant position angle, ~50°.[2] Recently published photometric polarimetry by Doroshenko, Efimov, & Shakhovski (1995) confirms this early trend and reveals a mild wavelength-dependent decline in polarization after the second maximum.

[1] It should be noted that the numbers from Smith (1993) have been corrected for statistical bias via the prescription of Wardle & Kronberg (1974) and that the reported numbers are consistent with zero observed polarization (e.g. Simmons & Stewart (1985).

[2] We strongly encourage polarization observations of other stars within the spiral arms of M81 to estimate independently the interstellar component within the spiral arm.

The spectropolarimetric data are thus a critical diagnostic for the models. The data of Jannuzi et al. (1993), Tran & Filippenko (1993), and Miller (1993) must be closely examined to check the degree of polarization and the position angle across Hα.

5. COMPARISON WITH OBSERVATIONS

The models can be compared with the observations of SN 1993J to show the potential of a simultaneous analysis of flux and polarization spectra and to show that the models may have some resemblance to reality. We seek qualitative agreement and restrict our considerations to quantities that will be little affected by NLTE. Our comparison is based on the observational data of Trammell et al. (1993). We have assumed an interstellar reddening E_{B-V} of 0.2 mag, substantially concentrated in M81 (Wheeler et al. 1993; Clocchiatti et al. 1995).

The effective temperature is a free parameter in our models that determines the overall slope of the flux. Best agreement with the observations is achieved for $T_{\rm eff}$ = 4800 K. Models with $T_{\rm eff}$ of 4500 and 5500 K do not fit the overall flux distribution.

Although the Hα line may be subject to departures from LTE, we treat it here in LTE. The flux spectra show a flat-topped Hα profile that may be related to the imminent onset of the He I λ6678 line that becomes noticeable less than a week after the epoch we consider or to the shell-like nature of the H envelope. We do not attempt to reproduce this detail. The absorption component of Hα shows evidence of a double minimum. This may suggest some contamination from Si II λ6355 (Wheeler et al. 1994). This feature may also be out of LTE, and we also do not attempt to reproduce the details of the absorption profile.

The flux spectra also show a broad, perhaps double, minimum at about 5700 Å. This feature can be approximately reproduced in the current models with a line of He I λ5876, but only with a very large enhancement of the opacity of that line, by a factor of 10^9 (Fig. 5).

The He is expected to be far out of LTE because of the lack of thermal photons and the presence of γ-radiation, but the required enhancement factor seems excessive. In their model for the April 20 spectrum, Swartz et al. find a strong gradient in the departure coefficients. Typical values for the

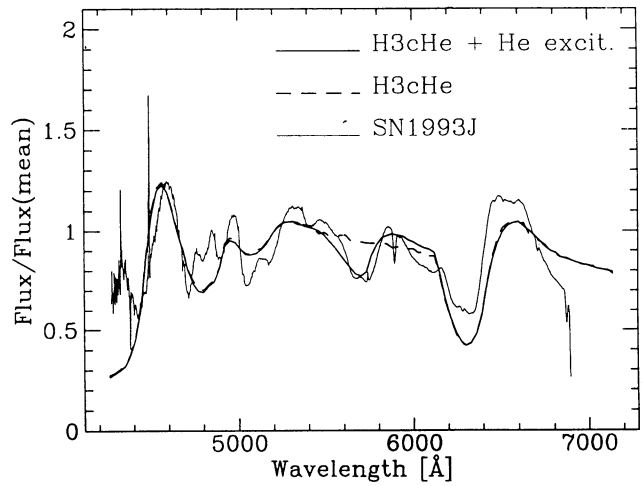

FIG. 5.—Flux of H3cHe with and without and enhanced He I (i = 90°) in comparison to observations of SN 1993J at 1993 April 21. E = 0.6, $T_{\rm eff}$ = 4800 K, $R_{\rm ph}$ = 1E15 cm.

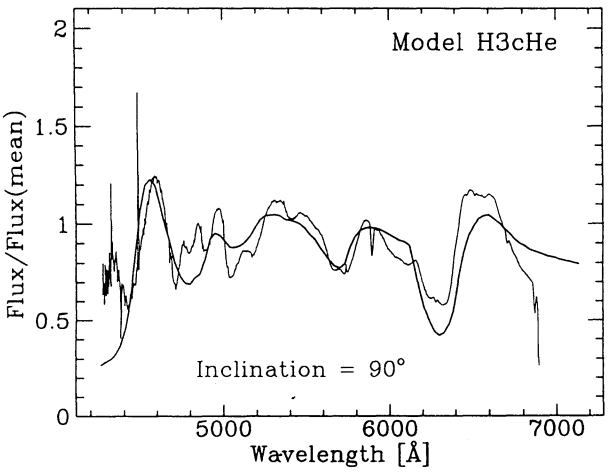

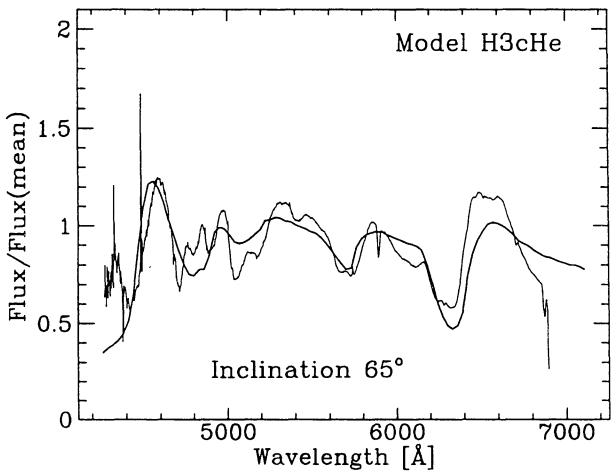

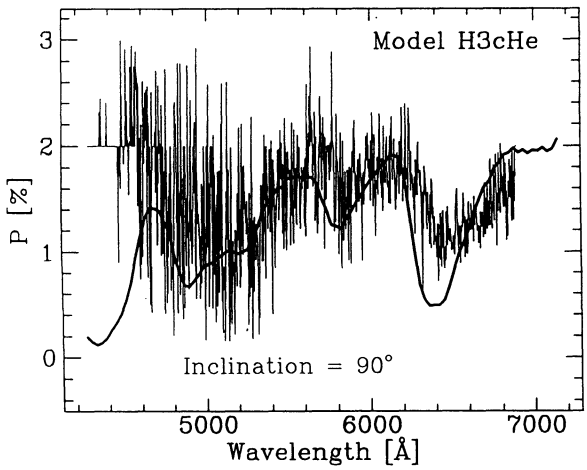

FIG. 6a

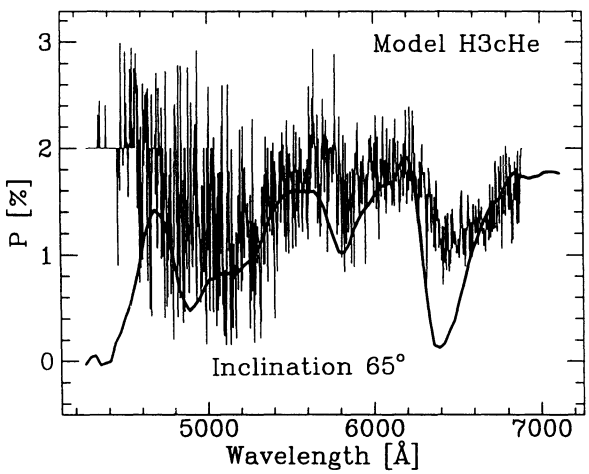

FIG. 6b

FIG. 6.—(*a*) Flux of H3cHe seen at an inclination of 90° in comparison to the spectrum of SN 1993J observed at 1993 April 21. (*b*) Same as (*a*) but $i = 65°$. (*c*) Same as (*a*) but $i = 30°$. $E = 0.6$, $T_{\rm eff} = 4800$ K, $R_{\rm ph} = 1E15$ cm.

first and second excited levels of He I (with higher levels having somewhat smaller values are 1.0×10^{12} at the base of the helium layer ($M_r = 0.7\ M_\odot$, $v = 3300$ km s^{-1}); 1.0×10^8 in the middle of the helium layer ($M_r = 1.5\ M_\odot$, $v = 5800$ km s^{-1}); 50 near the top of the helium layer ($M_r = 2.0\ M_\odot$, $v = 7500$ km s^{-1}); and unity in the middle of the H/He envelope layer ($M_r = 2.4\ M_\odot$, $v = 7500$ km s^{-1}). Although small variations in the electron temperature can change the LTE population numbers and hence the normalized departure coefficients significantly, it thus seems unlikely that large departure coefficients and hence large variation from LTE opacities, of order 10^9, exist in the H envelope.

As shown by Swartz et al. (1993), a consistent treatment of the γ-ray excitation in the rate equations gives a good representation of the spectra of April 29 and May 9 when the He I lines are clearly observed. The spectrum makes an obvious transition between April 20, when the current spectropolarimetric data were obtained, and April 29, when the He I lines begin to become apparent. In particular, the feature at 5700 Å develops a much stronger and sharp minimum that is clearly indicative of He I λ5876. It may be that the feature at 5700 Å in the April 20 spectrum that we analyze here did not contain any substantial component of He I but rather was comprised of Na D with perhaps some additional effect of Fe II lines. Nevertheless, in the current calculations the He I line has been included, and its effects on the polarization can be addressed. The qualitative conclusions may also pertain if the line were instead Na D, probably also subject to NLTE excitation.

The theoretical spectra of H3cHe are compared to the observations in Figure 6. By comparing the flux spectrum F_λ (*upper panels*) with the polarization spectrum P_λ (*lower panels*), one sees that the depolarizing effects of the Hα line are distributed over the whole P Cygni line profile. In both the observations and theory, the depolarization sets in steeply somewhat to the red of the blue edge of the absorption, reaches a minimum slightly to the red of the absorption minimum, and then rises more slowly through the rest frame wavelength P Cygni peak and into the red wing of the line. The polarization profile is "out of phase" with respect to the flux profile since depolarizing requires only a single line scattering, but several scatterings are required to substantially alter the flux. At the Hα minimum of the polarization spectrum $P_\lambda \sim 1\%$. This value represents the continuum polarization since the process of correcting the observed spectra for effects of the ISM adopted by Trammell et al. involved the assumption that there is no polarization in the Hα line itself at the rest wavelength.

If viewed from the equatorial plane ($i = 90°$), the theoretical absorption components of the line fluxes for model H3cHe are significantly too broad, although at the right

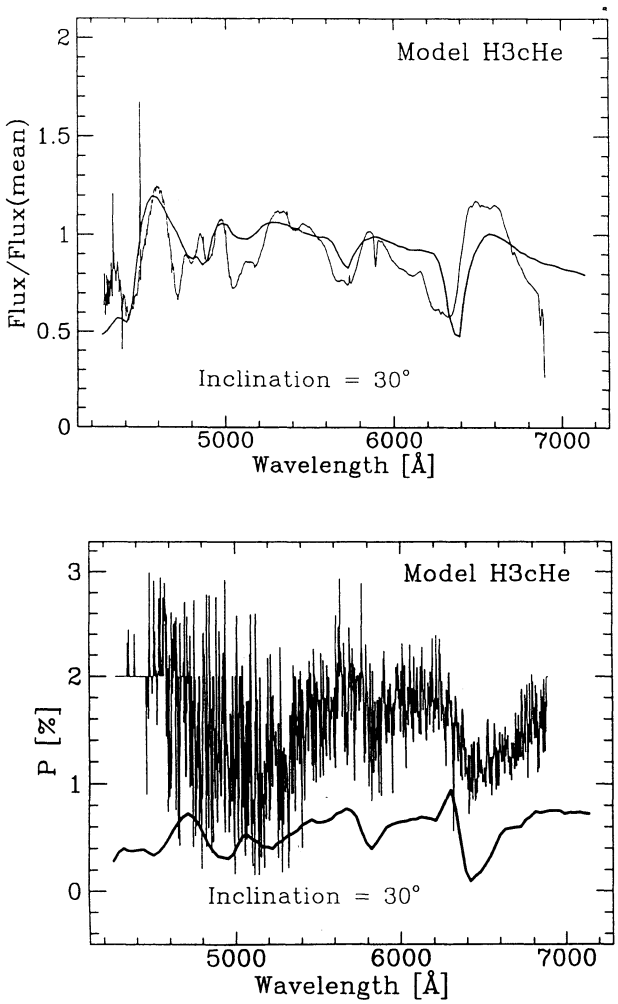

FIG. 6c

frequency shift. In general, the polarization spectrum provides the right amplitude for the percentage polarization, P_λ. The blue wing of Hα extends too far by about 200 Å. The depolarization over the "He I" line at ~5700 Å is about correct. For this model, both P_λ and F_λ show the need for smaller inclination.

At $i = 30°$ (Fig. 6c), the flux profiles tend to be too narrow, and the Doppler shift of the absorption component becomes too small. The differences in the flux spectrum may be corrected by choosing a larger outer radius (i.e., a somewhat larger expansion velocity), but then the amplitude of P_λ, which is already too small in Figure 6c, would decrease even further because of enhanced multiple scattering.

For oblate models, the depolarization in Hα increases as the inclination decreases because as the line of sight moves toward the symmetry axis, there is a steeper density gradient and hence an increase of the depolarizing effects of multiple scattering compared to Thomson scattering. This effect will occur at any density gradient, but its amplitude will depend on the value of the density gradient. In Figure 6c, P_λ at the absorption minimum of Hα essentially vanishes, in strong disagreement with the observations. This is because, in this model, the optical depth for line scattering is so high compared to Thomson scattering that even the residual continuum polarization from the more nearly symmetrical geometry is removed by depolarizing effects of line scattering.

In principle, the absolute polarization in the continuum could be increased with larger asphericity. The fact that $P_\lambda \sim 0$ at the absorption minimum of Hα is not likely to change with moderate increase of asphericity and hence this problem cannot be fixed in that way. The excessively small polarization at Hα might be adjusted if the adopted polarization of the ISM were incorrect. As discussed below, there is no evidence that the applied correction is substantially in error, and altering that correction would not change the relative degree of depolarization at Hα compared to shorter wavelengths. In fact, the depolarization at wavelengths below 5400 Å is too weak compared to Hα, and this problem would remain if there were a simple renormalization associated with a different ISM polarization component.

Thus, although some parameters could be adjusted to improve certain aspects of the calculation, we conclude from the model H3cHe that small inclinations are not consistent with SN 1993J.

A medium inclination $i = 65°$ alleviates some problems with respect to the flux spectra but suffers both the problems with excessive depolarization in Hα that plague $i = 30°$ and the overly broad absorption components in F_λ that occur for larger i. Overall, models with excessively low density gradients, $n \lesssim 3$, are not acceptable.

For the flux spectra, better agreement with the observations can be achieved for power-law densities with $n = 5$–7 (Figs. 7 and 8). Further adjustment of parameters might result in closer agreement. We forego this exercise because the limits of the models would prevent gaining much additional information.

The polarization spectrum shows that H7cHe also has some problems (Fig. 7). In particular, Hα is significantly too narrow by almost a factor of 2. For steep density gradients, the wavelength range with significant optical depth is very restricted. This problem becomes more severe for models with even steeper density gradients and corresponding smaller scale heights. The polarization spectrum, in particular, puts an upper limit on the density gradient in SN 1993J. Models with $n \gtrsim 7$ do not give acceptable agreement with the observations.

A reasonable fit to both the flux and polarization spectra is provided by H5cHe at high inclinations. Since the absolute degree of depolarization becomes too strong for low inclinations (see above), we conclude that the inclination should be larger than about 65° and is probably close to 90°. With this combination, both F_λ and P_λ for SN 1993J are reproduced reasonably well.

6. DISCUSSION AND CONCLUSIONS

A new version of our Monte Carlo code is presented which allows the calculations of polarization and flux spectra for arbitrary three-dimensional geometries in rapidly expanding envelopes if the temperature, velocity, and density structure are given. Calculations using this code for scattering-dominated, rapidly expanding photospheres have been performed to study the influence of deviations from sphericity on the spectra and polarization of SN 1993J.

6.1. *Implications for Distance Determinations*

We have shown that deviations from sphericity as high as a factor of 2 are difficult to detect by analysis of spectral fluxes alone. Although the flux depends sensitively on the

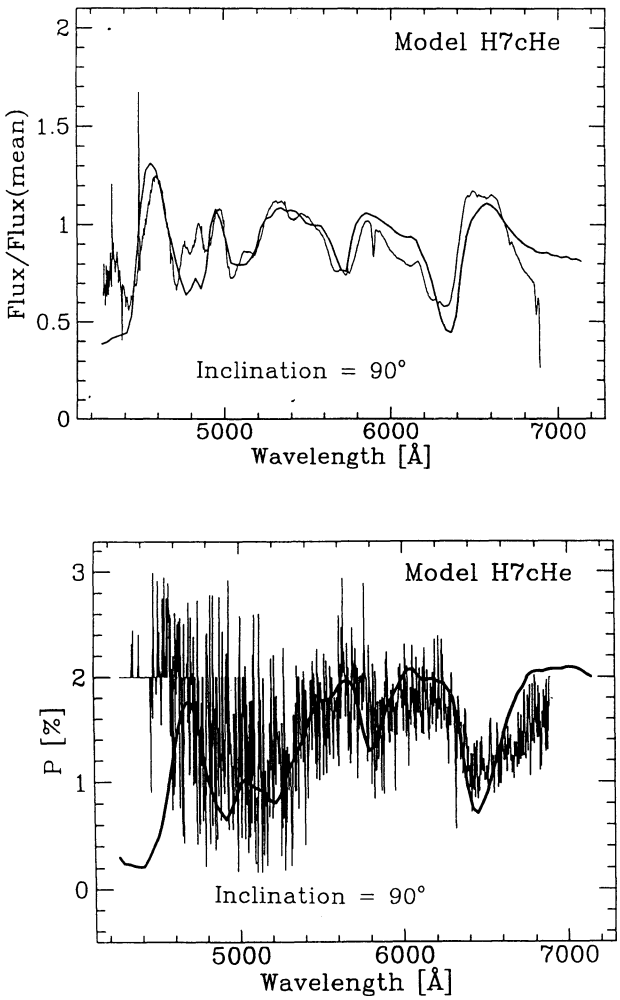

FIG. 7.—Flux H7cHe seen at an inclination of 90° in comparison with the spectrum of SN 1993J at 1993 April 21. $E = 0.6$, $T_{\rm eff} = 4800$ K, $R_{\rm ph} =$ 1E15 cm.

direction from which an envelope is observed, it is possible to find a set of parameters for a corresponding spherical model that reproduces the observations. Note that a similar result has been found for static, isothermal envelopes by Schmid-Burgk (1982) for the continuum problem.

Since observed spectra of an aspherical supernova can be reproduced by spherical models with the adjustment of free parameters such as the stellar radius or by introducing a small microturbulence, we cannot draw accurate conclusions about the geometry of a given supernova based solely upon the flux density spectrum. Even in the case of very well observed supernovae such as SN 1987A, asphericities of the order of 10%–20% may remain undetected if no polarization measurements are available. This conclusion has implications not just for our understanding of supernova explosions and the progenitor evolution but also for the use of SN II's as distance indicators. Asphericity intrinsically demands a direction dependence of the deduced intrinsic luminosity. The application of the expanding photosphere method to Type II supernovae in particular must treated with care.

6.2. *Effect of Density Gradient and Inclination*

The sensitivity of polarization spectra to the underlying density structure and the inclination angle i has been demonstrated. The polarization provides a good test of the optical depth in a line, since photons are depolarized even by moderate τ. On the other hand, the intrinsic polarization does not necessarily vanish over strong lines such as Hα because of Thomson scattering within the line-forming region. Depolarization by many lines in a broad wavelength range is as effective as a single strong line, but regions of moderate optical depth in the individual weak lines are more geometrically compact. This, in turn, lowers the effective contribution of Thomson scattering and the residual polarization. The ratio between depolarization caused by single, strong lines to that by multiple lines of moderate opacity thus provides additional information, e.g., about the density structure.

The observations of SN 1993J have been reanalyzed using the polarization and flux spectra of Trammell et al. (1993). For the oblate models studied here, we find that the best agreement with observations occurs for power-law index n of the density gradient ($\rho \propto r^{-n}$) at the line-forming region in the range $3 \lesssim n \lesssim 7$ with a best value of about $n = 5$. The flux spectra also suggest that the density gradient cannot be too steep, but the polarization gives more stringent limits.

Although we have not varied the ellipsoid axis ratio E in this study, a value of 0.6 produces results in reasonable quantitative agreement with previous investigations (Höflich 1994). If oblate ellipsoidal geometry holds for the envelope structure of SN 1993J, we can infer that SN 1993J was seen "equator-on." Oblate models give more polarization when viewed on the equator for two reasons that act in the same direction. The first reason is that the geometrical effect of the distortion from spherical symmetry is maximized along the equator. The second effect is that the depolarizing effects of line scattering versus Thomson scattering are minimized for equatorial lines of sight because of the shallower density gradient and lower photospheric density.

We have not explicitly studied prolate geometries here. For prolate models, the effect of geometry on polarization is again maximized by viewing along the equator. The depolarizing effects of line scattering are, however, also maximized because now the steepest density gradients and photospheric densities are along the equatorial, not the polar, direction. This is why, in general, such prolate geometries would require higher distortions (smaller values of the axis ratio E) to reproduce a given degree of polarization. Quantitative constraints on the density gradient and inclination angle of prolate models would require specific numerical models that we have not done here. We believe that adopting prolate geometries would not substantially alter our conclusion that density gradients can be neither too steep nor too shallow nor our conclusion that SN 1993J was observed approximately normal to the symmetry axis.

6.3. *Determination of the Interstellar Polarization Component*

The problem of the interstellar component of the polarization can be reexamined in the context of our results. The procedure adopted by Trammell et al. (1993) to evaluate the ISM component involved the formal assumption that the polarization at Hα consisted of supernova continuum, an added Serkowski law component imposed by the ISM in M81, and the contribution from Hα itself. The implicit assumption was that a polarized continuum emerged from a deep layer, then passed through the H-scattering layer, and

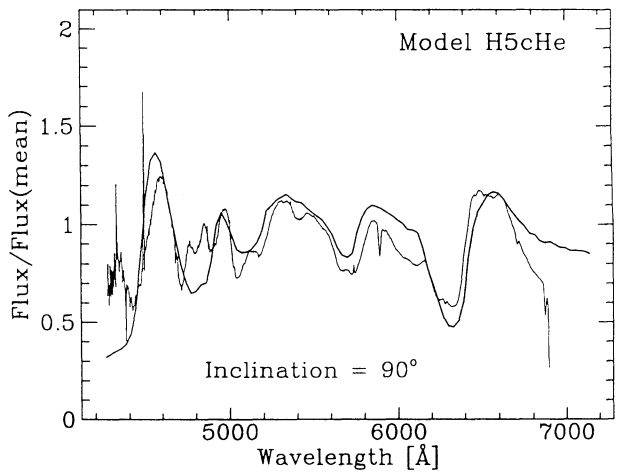

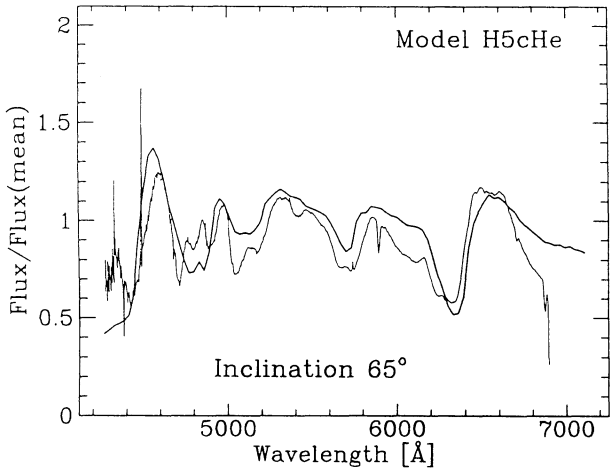

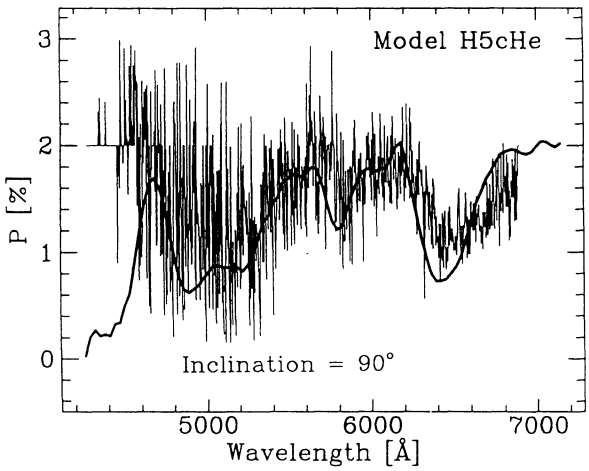

FIG. 8*a*

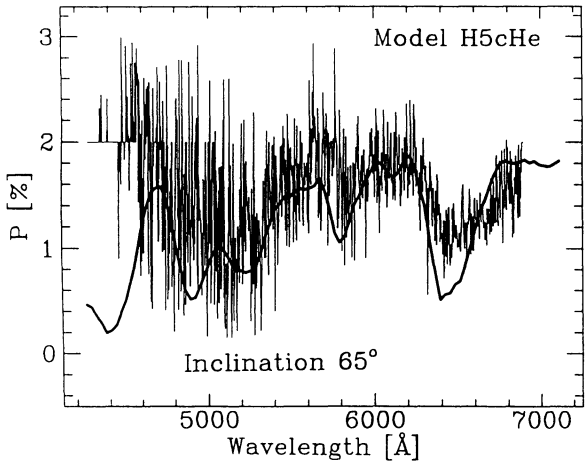

FIG. 8*b*

FIG. 8.—(*a*) Flux H5cHe seen at an inclination of 90° in comparison with the spectrum of SN 1993J at 1993 April 21. (*b*) Same as (*a*) but $i = 65°$. (*c*) Same as (*a*) but $i = 30°$. $E = 0.6$, $T_{\rm eff} = 4800$ K, $R_{\rm ph} = 1E15$ cm.

then passed through the ISM. This allowed the three components to be combined by vector linear addition. In reality the interaction of the continuum and lines is more complex. Trammell et al. took the intrinsic polarization of the Hα line to be zero and assumed that the intrinsic continuum polarization from the supernova is continuous so that its value at Hα could be determined by interpolation from the surrounding continuum. This allowed them to subtract the continuum contribution at Hα and to assume that the remaining polarization at Hα gave the amplitude and orientation of the ISM.

The assumptions that the continuum can be interpolated and that only continuum electron scattering and the ISM contribute at Hα may not be correct (e.g., Schmidt 1995; Tran & Filippenko 1993). We see from the models, especially those that are viewed nearly pole-on, that the strong depolarizing effects of the line scattering can depolarize the continuum so that the continuum at line center cannot be evaluated by interpolation. In other circumstances, some continuum polarization may be added at Hα since scattering electrons are present in the line-scattering region. The continuum polarization is not necessarily determined in a layer completely beneath the H layer.

Although these caveats must be carefully considered and reevaluated if new data become available, the current models suggest that the ISM has been correctly removed from the polarization spectral data presented here (Figs. 6, 7, and 8). These models reproduce the line profiles in terms of the breadth of absorption components, the amplitude compared to the continuum, and the line shifts for both F_λ and P_λ. The differing amounts of depolarization between different wavelength regions can also be reproduced. In addition to the flux distribution given by $T_{\rm eff}$, we have adjusted $v_{\rm ph}$, n, and i. The ellipsoid axis ratio E is given by the absolute size of P_λ, and $R_{\rm ph}$ follows directly from $v_{\rm ph}$ and the time of explosion. Significantly larger distortion (smaller E) would require a smaller inclination angle i that can be excluded from the polarization spectrum over Hα.

We conclude that the ISM correction suggested by Trammell et al. (1993) is likely close to reality. Determining the interstellar component from a measured polarization may be difficult in general without additional information such as the position angle as a function of wavelength and, as for the case of SN 1993J, the magnetic field structure within the spiral arms of M81. In principle, the technique outlined in this paper can be used to determine iteratively

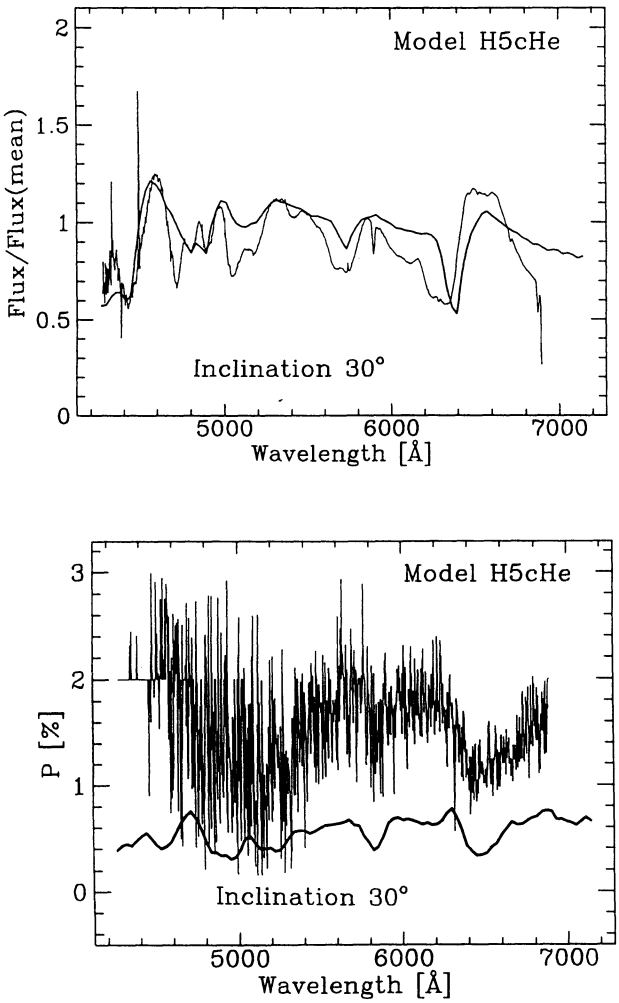

FIG. 8c

the interstellar component independently of other estimates.

6.4. *Constraints on Dynamic Models*

This analysis of the polarization allows us to reexamine the dynamical models for SN 1993J in a new perspective. One of the significant controversies about the nature of the explosion in SN 1993J is the question of when the photosphere receded from the outer hydrogen layer into the inner helium mantle. The various points of view are summarized in Wheeler & Filippenko (1995). In models with small ejecta mass, ~ 1.6–$4.6\ M_\odot$, modest hydrogen envelopes, ~ 0.1–$1\ M_\odot$, and little outward mixing of radioactive nickel, the photosphere recedes into the helium layer at the first minimum of the light curve about 7 days after the explosion (Wheeler et al. 1993; Woosley et al. 1994). The models of Wheeler et al. with no nickel mixing did a good job of matching the V magnitude through the second peak but found the photosphere to recede rapidly through the relatively cold and neutral helium and into the C/O mantle. This resulted in too rapid an evolution to the blue after the first minimum. Woosley et al. invoked a modest mixing of Ni outward, and the photosphere was held in the helium layer until near the second maximum. Models by Shigeyama et al. (1994) and Höflich et al. showed the photosphere lingering in the hydrogen envelope until near the second peak. Shigeyama et al. invoked an ejecta mass comparable to that of Wheeler et al. and Woosley et al. but assumed a considerable amount of Ni mixing. This may not be allowed since if the hydrogen is too strongly exposed to the radioactive decay, it will be overionized and the H lines will be too weak (Swartz et al. 1993). Höflich et al. have explored models at the extremes of rather low ($10\ M_\odot$) and rather high ($30\ M_\odot$) main-sequence mass and found that the low-mass models were strongly contradicted by both the observed spectra and light curves because of the lack of a massive inner C/O core. The more massive models of Höflich et al. contained about (~ 11 and $3\ M_\odot$ in the ejecta and hydrogen envelope, respectively, and also invoked extensive outward mixing of Ni. The initial and final mass ejected by SN 1993J is probably somewhat lower (see below).

There are several reasons to believe that, despite other possible quantitative problems (e.g., interstellar reddening), the models of Shigeyama et al. and Höflich et al. are qualitatively correct in the statement that the photosphere did not recede into the helium layer until near the second maximum. One of these is the color evolution. The $B-V$ color reddened during the first decline to minimum. The color was relatively flat during the subsequent rise to the second maximum, at which point it evolved rapidly redder again. The color plateau on the second rise is not easy to explain. Wheeler & Filippenko suggest that it might represent a phase at which the photosphere is trapped in the helium layer (by radioactive heating) and at which the subsequent reddening is when the photosphere finally recedes into the metal core. This may not be consistent with the spectral evolution. The helium lines were not observed until just before the second maximum (Swartz et al. 1993; Filippenko, Matheson, & Ho 1993). It is possible, but probably not likely, that the photosphere had receded into the helium during the rise but not sufficiently that strong helium lines were produced. Such a situation would seem to require too much "fine tuning." The spectral models of Swartz et al. require the photosphere to be in the hydrogen layer on April 20, when the current spectropolarimetry was obtained, and then recede into the helium layer by April 29 when the He I lines were distinctly observed in the optical and IR. Utrobin (1995) gets reasonable results for the emergence of the helium lines with a model of $2.4\ M_\odot$ total ejecta of which the outer $2\ M_\odot$ is He fully mixed with about $0.1\ M_\odot$ of H. There is no pure helium mantle, in contrast to the results of most evolutionary calculations. In these models, the nickel is confined to the inner layers of heavy elements. Despite lingering problems with the color evolution on the second rise, Utrobin's models provide an interesting alternative to high-mass hydrogen-rich envelopes and combine some of the advantages of both the high-mass and low-mass models outlined above.

The polarimetry gives another perspective on this issue. If the analysis of the results from Bjorkman & Nordsiek (1993) and from Smith (1993) presented here (§ 4) are taken at face value, then the polarization did not change its orientation nor value at the time of the first minimum. This suggests that there was not a major change in the structure of the atmosphere at that time. Rather than a recession of the photosphere into the helium layer, this may have just been a time of transition from adiabatic cooling by shock heating to heating by the interior radioactive decay.

The quantities P_λ and F_λ measure different physical effects (see above) and, consequently, different layers of the

expanding envelope. Both the polarization and flux spectra presented here are consistent with the photosphere still being in the hydrogen layer on April 20, 3 weeks after the explosion. The models are consistent with nearly the same expansion velocity for the Hα and "He I" lines despite rather different optical depths, ~100 and 10 for Hα and He I, respectively. This evidence for homogeneity of composition may need reevaluation if the relevant feature is not He, but Na.

Test calculations in which He has been substituted for H up to $2R_{ph}$ to test whether the photosphere could be in a helium mantle in late April gave poor results. The H profile becomes overly boxy in both absorption and emission and in the polarization profile. The amount of polarization also drops because there are fewer free electrons to scatter in the pure helium layers. This could be overcome by increasing the distortion of the geometry, but this would then demand a correspondingly larger polarization in the earlier observations when the photosphere was definitely in the H envelope. It seems unlikely that the distortion grows inward, but perhaps this cannot be ruled out. The models in which the photosphere remains in the hydrogen layer until after day 20 are qualitatively consistent with the small increase in derived polarization since the photosphere will recede to deeper layers where the density gradients tend to be less and hence depolarization is decreased. Qualitatively, the present results agree with those of Swartz et al. 1993 (see also Baron et al. 1993, 1994) that on April 20 the photosphere is still formed in the H/He rich layers.

The models presented here put constraints on the gradient of the density at the photosphere. The present results show that a gradient steeper than $n = 7$ is not consistent with the current models and observations and that $n = 5$ is preferred. This puts constraints on the structure of the dynamical model and perhaps on the interaction with the circumstellar medium. The explosion of a star with an initial structure resembling a polytrope of index 3 will give a postshock structure with a slope $n \sim 7$. On the other hand, an initial structure with a fairly massive (comparable to the core mass) extended envelope will yield a postexplosion structure with the envelope compacted into a shell with a very steep density gradient on the outer face. Models of SN 1987A gave density gradients with $n \sim 3$ near the base of the H envelope. Moderate-mass models for SN 1993J (Shigeyama et al. 1994) give $n \sim 20$–25 in the very outermost layers but closer to $n = 3$ in the bulk of the H envelope and into the helium mantle. Clocchiatti et al. (1995) conclude that the photosphere did have a steep density gradient in the very early phases, but the current observations pertain to several weeks after maximum. There dynamical models are more consistent with a modest density gradient as we have derived here. Baron et al. (1993, 1994) consider exponential atmospheres and suggest that the gradient must have an equivalent density index of $n = 12$–23 at this phase. This does not seem to be consistent with the dynamical models nor the results derived here.

6.5. *The Origin of the Polarization*

The preeminent question raised by this work is the cause of the distortions that lead to the polarization. To put this question in perspective we must examine both the nature of the polarization and its time dependence.

Trammell et al. (1993) suggested that the flux from a scattering layer above the photosphere is already polarized as it impinges on the hydrogen envelope from below. This flux was then envisaged to be absorbed upon passage through the hydrogen layer. This physical picture, which was implicit in their mode of analysis and decomposition of the polarized flux into continuum, line, and ISM effects, was supported by the form of the derived Stokes flux. The Stokes flux showed a blueshifted absorption component, which suggested that the polarization was already imposed on the continuum at deeper layers and then some of the polarized flux was scattered or absorbed as it passed through the hydrogen layer.

An important result of the models presented in this paper is to illustrate that the simple idea of a polarized continuum flux impinging on the hydrogen layer from below may be both simplistic and incorrect. The reality is more complex. Trammell et al. questioned whether the polarization could both be generated within the H layer and still have enough optical depth to do the requisite "absorption" that is observed in the polarized flux density spectrum. The current models show that the polarized continuum and the depolarization of the line can be generated in the same layer. The shape of the absorption trough in the polarization spectrum, the percent polarization, presented here is roughly consistent with this.

The interpretation of Trammell et al. also has the drawback that if the scattering layer is beneath the H envelope, the large intrinsic polarization requires that the very large distortions, with axis ratios of order 1.5–1 or $E \sim 0.6$ (Shapiro & Sutherland 1982; Trammell et al. 1993), must be in the helium core. This level of polarization is difficult to generate and maintain in polytropes strongly distorted by differential rotation (Steinmetz & Höflich 1992) or by aspherical explosions in basically spherical core/envelope configurations because sphericity tends to be regained in the expansion.

Another constraint on this interpretation is provided by the analysis of Höflich (1994). In simple parameterized models with distorted cores and spherical envelopes, Höflich finds that the polarization is low as long as the spherical envelope is optically thick. As the photosphere recedes, the polarization grows to the large values dictated by the distortion of the core, even suffering a reversal of sign since the long axis will emerge from the optically thick envelope before the short axis. No such strong time dependence is seen near the first minimum or near the second maximum in the light curve, the two suggested times when the photosphere might recede from the envelope to the core. It thus seems difficult to reconcile the hypothesis of a distorted core and spherical envelope with the relatively weak time dependence of the polarization.

An alternative possibility is that the flux from the core is unpolarized and that a nonspherical configuration in the envelope creates the polarization through scattering. This is the basic *Ansatz* that is assumed for the models presented in this paper. A distorted envelope is not out of the question, given the evidence in many other contexts for bipolar flow associated with late stages of evolution, especially in binary systems. An advantage of this picture is that with a configuration in which an unpolarized, nearby point source (the core) illuminates a distorted scattering envelope, much less distortion is required to produce the same degree of polarization (Brown & McLean 1977; Fox 1991; Höflich 1991a; Trammell et al. 1993).

A distorted envelope probably requires some mechanism other than rapid rotation since the envelope is expected to be extended and convective. Höflich (1994) has argued that a binary common envelope configuration, in particular, may naturally yield the necessary distorted envelope. We also note that with the understanding that the Hα profile is distorted somewhat by He I λ6678, there is no direct evidence in the spectrum at this epoch for any major asymmetries in the envelope. As noted above, however, this does not assure that the envelope is spherically symmetric.

Höflich (1994a) argues that the polarization should be nearly constant while the photosphere is in the distorted envelope. This is consistent at some level with the observations from early April to April 20. The slow rise suggested for this interval could be due to the effect of the flattening density gradient. It is not clear, however, that this model can account for the observations of Jannuzi et al. (1993). The close agreement of the observed size and orientation of the polarization between the results of Trammell et al. (1993) and of Jannuzi et al. gives a reassuring self-consistency but may provide a stringent test of models.

The important difference is that the observations of Trammell et al. on April 20 were very likely made while the photosphere was still in the hydrogen envelope, given the lack of evidence for strong lines of He I, as discussed above. The observations of Jannuzi et al. were made only 6 days later, April 26, but this was a critical week in the spectral evolution of SN 1993J. The He I lines, especially He λ6678, began to appear between April 22 and April 26 (Hu et al. 1993; Swartz et al. 1993; Filippenko et al. 1993; Wheeler & Filippenko 1995). Thus the observations of Trammell et al. were probably made just before the photosphere receded into the inner helium mantle and those of Jannuzi et al. just after this transition. It is thus remarkable that the results of Trammell et al. were similar to the polarization determined near the first minimum and especially that there was no significant change in the amplitude and orientation of the polarization between April 20 and April 26. We do note that the small rotation $\sim 10°$ across Hα in the data of Trammell et al. becomes a $\sim 20°$ rotation in the Steward data, even after correction for the interstellar polarization (Schmidt 1995). This may be a signature of the photospheric transition, but it is rather subtle. It is not clear that the overall constancy of the polarization amplitude and angle can be reconciled with notion that the polarization is due to a distorted hydrogen envelope and that the photosphere receded through the base of the hydrogen envelope at this time. Höflich suggests that envelope distortion could be caused by a common envelope configuration in which the companion was close to the inner edge of the hydrogen envelope. It is difficult to see how the effects of such a companion, in the polarimetry or otherwise, would not be seen very distinctly at this epoch.

One might argue that the photosphere was sufficiently deep in the hydrogen envelope even at the time of the Trammell et al. observations that there was no change in the polarized component despite the change in the total spectral features as the photosphere receded on into the helium layers. This is difficult to reconcile with the fact that the polarization observed on April 4–7 (corrected for ISP), when the photosphere was in the outer portions of the hydrogen envelope, was essentially the same as on April 20–26 when the photosphere was near the base of the hydrogen. In the former case, the envelope was still optically thick, while in the latter, it was optically thin; yet this seems not to have affected the polarization significantly.

Höflich (1994) also explores a model in which the geometry is spherical but in which the emitted light is polarized because the source of the radiation, perhaps a pulsar or a blob of radioactive nickel, is off-center. This model might be consistent with the surprisingly circular shape of the VLA radio image (Bartel et al. 1994). Höflich notes that for consistency of this model with SN 1993J, the source of the asymmetric flux must have been at large optical depth even at the end of April, that is, within layers that were still optically thick even though the hydrogen layer was rapidly becoming optically thin. A continuum was observed in SN 1993J until at least 1993 June, which suggests that some portions of the ejecta were still optically thick at that time and that the velocity of the photosphere was well above 1000 km s^{-1}. Thus, an asymmetric energy source could still be buried for some time. This picture may be consistent at some level with the near constancy of the polarization from early to late April. Although the polarization varies strongly with optical depth for moderate to small optical depth (Höflich 1990), it varies only slowly with optical depth for a buried asymmetric source. There should be a strong variation of the polarization as any asymmetric source finally becomes exposed. The later Lick data may put important constraints on this hypothesis. At the current epoch, 2 years later, there is no sign of a pulsar, buried or otherwise, but asymmetries of the nebular emission lines may be consistent with a strongly off-center blob of radioactive nickel (Chugai & Wang 1996).

We are left with the conclusion that while the current models have given some important constraints on the size of the asymmetry and the orientation, we do not have a clear picture of how the polarization is physically generated. In particular, it is difficult to see how any model can give nearly constant polarization in amplitude and orientation, from early April when the hydrogen-rich envelope was optically thick to late April when it was optically thin. In hindsight, the observations, sparse as they are, were ideally timed. The early observations span the first minimum. If that were the time when the photosphere receded from the hydrogen to helium layers, then some change in polarization might be expected, yet none was apparently observed. The observations in late April span the time when the spectrum became helium rich, which strongly suggests that the photosphere receded from the hydrogen to the helium layers. The constancy of the polarization is even more reliable at this epoch. It is difficult to see how distorted cores or envelopes could give this behavior. An asymmetric source of the flux might be consistent with the data of the first month.

It is perhaps also worthwhile to consider other means of generating the observed polarization. One factor that has not been investigated quantitatively here is the circumstellar medium. We know that such a medium is present from its effects on the radio and X-ray emission and the continued emission of Hα. Scattering from an external medium might give the nearly constant polarization observed, or at least contribute to the total polarization in a way that has yet not been considered. The residual rotation of the polarization at Hα after correction for the ISM in the Arizona data suggests that the line emission region has a slightly different geometry than the continuum and hence that there is some factor involved beyond the ISM and the electron-

scattering component of the supernova ejecta. Spectropolarimetry of Nova Cas 1993 (Trammell et al. 1993) shows that P Cygni line profiles generated in the nova ejecta are scattered and polarized by an external medium, probably dust rich, that is receding from the nova at about 200 km s^{-1}. In this object, at least, there is clear evidence that the scatterers are located exterior to the absorption in the lines, in the spirit of the original suggestion of Trammell et al. (1993). There is the potential for such an effect in the circumstellar nebula of SN 1993J. In particular we note that dust scattering is wavelength independent, like electron scattering, but of order 100 times more efficient at scattering.

There are, however, several problems with invoking the circumstellar medium to account for the observations of SN 1993J. It would be very difficult for an aspherical wind to produce a significant total polarization because of the expected small optical depth to electron scattering, although dust scattering might be significant if the matter is dusty. Another important factor is that the broad minimum in the polarization spectrum presented here must obviously be formed in the supernova ejecta, not by Hα absorption in any external medium. It may nevertheless be conceivable that an external scattering screen could be exposed to relatively more of the continuum-emitting volume than the Hα-emitting volume because of optical depth effects within the ejecta. Whether this sort of configuration could reproduce the observed polarization as well as the models presented here requires quantitative investigation.

To understand the nearly constant polarization and the rotation of the polarization at Hα, to check the current models, and to explore the possible effect of an external dust scattering medium, it becomes even more imperative to closely examine the later data obtained at Steward and Lick Observatories.

The other main question remaining to be answered is whether deviations from sphericity are quite common for SN II's or whether SN 1987A and SN 1993J were "bad luck." The answer to this question is critical if SN II's are to be used as standard candles. We strongly recommend that polarization measurements of supernovae be obtained on a regular basis.

P. A. H. takes great pleasure in thanking Bob Kirshner and all the members of his group for helpful discussions and useful comments. Special thanks go to Al Cameron for his support. J. C. W. is grateful to Lifan Wang and Alex Lazarian for reading the manuscript and for helpful comments. This work has been supported by the Deutsche Forschungsgemeinschaft through the grant Ho 1177/2-1, by NSF grant AST 92-18035, and by NASA grant NAGW 2905. Some of the computations were performed at NCSA under the grant AST 94-0002N.

REFERENCES

Abbot, D. C., & Lucy, L. B. 1985, ApJ, 288, 679
Arnett, W. D., Bahcall, J. N., Kirshner, R. P., & Woosley, S. E. 1989, ARA&A, 27, 629
Baade, W. 1926, Astron. Nachr., 228, 359
Baron, E., Hauschildt, P. H., & Branch, D. 1994, ApJ, 426, 334
Baron, E., Hauschildt, P. H., Branch, D., Wagner, R. M., Austin, S. J., Filippenko, A. V., & Matheson, T. 1993, ApJ, 416, L21
Baron, E., Hauschildt, P., & Young, T. R. 1995, Phys. Rep., 256, 33
Bartel, N., et al. 1994, Nature, 368, 610
Baschek, R., Scholz, M., & Wehrse, R. 1991, A&A, 246, 374
Bjorkman, K., & Nordsiek, K. 1993, private communication with J. C. Wheeler; see also Wheeler & Filippenko (1995)
Branch, D., Falk, S., McCall, M., Rybicki, P., Uomoto, A. K., & Wills, B. J. 1981, ApJ, 244,780
Brown, J. C., & McLean, I. S. 1977, A&A, 57, 141
Chugai, N., & Wang, L. 1996, in preparation
Clocchiatti, A., Méndez, M., Benvenuto, O., Feinstein, C., Marraco, H., García, B., & Morrell, N. 1988, in Proc. of the 4th George Mason Conference on SN 1987A, ed. M. Kafatos & A. Michalitsianos (Cambridge: Cambridge Univ. Press), 70
Clocchiatti, A., Wheeler, J. C., Barker, E. S., Filippenko, A. V., Matheson, T., & Leibert, J. W. 1995, ApJ, 446, 167
Cropper, M. S., et al. 1987, MNRAS, 231, 695
Daniel J. Y. 1982, A&A, 86, 198
Doroshenko, V. T., Efimov, Y. S., & Shakhovskoi, N. M. 1995, Astron. Lett., 21, 513
Duschinger, M., Branch, D., Höflich, P., Kudritzki, R. P., & Puls, J. 1994, A&A, in press
Eastman, R., & Kirshner, P. R. 1989, ApJ, 347, 771
Filippenko, A. V., Matheson, T., & Ho, L. C. 1993, ApJ, 415, L103
Fox, G. K. 1991, ApJ, 379, 663
Fransson C., Lundqvist, P., & Chevalier R.A. 1996, ApJ, in press
Harkness, R. P. 1991, in SN 1987A and Other Supernovae, ed. J. Danziger & K. Kjär (Garching: ESO), 447
Hershkowitz, S., Lindner, E., & Wagoner, R. V. 1986, A&A, 301, 220
Hillebrandt, W., & Höflich, P. 1990, Rep. Prog. Phys., 52, 1421
Höflich P. 1988, Proc. Astron. Soc. Australia, 7, 434
———. 1989, in Particle Astrophysics, ed. E. B. Norman (Singapore: World Scientific), 205
———. 1990, Analysis of Type II Supernovae at the Photospheric Phase, Munich, Habilitation Thesis (MPA 563)
———. 1991a, A&A, 246, 481
———. 1991b, in Supernovae, ed. S. E. Woosley (New York: Springer), 415
———. 1994, A&A, in press
———. 1995, ApJ, 443, 89
Höflich, P., Langer, N., & Duschinger, M. 1993, A&A, 275, L29
Höflich, P., & Steinmetz, M. 1991, in Proc. 5th Workshop on Nuclear Astrophysics, ed. W. Hillebrandt & E. Müller (Garching: MPI), 103
Höflich, P., Wehrse, R., & Shaviv, G. 1986, A&A, 163, 105
Hu, J. Y., Li, Z. W., Jiang, X. J., & Wang, I. F. 1993, IAU Circ., 5777
Januzzi, B., Schmidt, G. D., Elston, R. E., & Smith, P. 1993, IAU Circ., 5776
Jeffery D. J. 1991, ApJ, 375, 264
Jeffery, D. J., et al. 1994, ApJ, 421, L27
Kraus, M., Beck, R., & Hummel, E. 1989, A&A, 217, 17
Lucy, L. B. 1988, in Proc. of the 4th George Mason Conference on SN 1987A, ed. M. Kafatos & A. Michalitsianos (Cambridge: Cambridge Univ. Press), 323
McCall, M. L. 1985, in Supernovae as Distance Indicators, ed. N. Bartel (Berlin: Springer), 48
McCall, M. L., Reid, N., Bessell, M. S., & Wickramasinghe, D. 1984, MNRAS, 210, 83
Méndez, M., Clocchiatti, A., Benvenuto, O. G., Feinstein, C., & Marraco, H. G. 1988, ApJ, 334, 295
Mihalas, D. 1978, Stellar Atmospheres (2d ed.; San Francisco: Freeman)
Miller, J. 1993, private communication
Miller, J. S., & Goodrich, R. W. 1990, ApJ, 355, 456
Schmid-Burgk, J. 1982, A&A, 108, 169
Schmidt, B., Kirshner, R. P., Eastman, R. G., Phillips, M. M., Suntzeff, N. B., Hamuy, M., Maza, J., & Aviles, R. 1994, ApJ, 432, 42
Schmidt, G. 1995, private communication
Serkowski, K. 1970, ApJ, 160, 1083
Shakhovskoi, N. M., & Efimov, Yu. S. 1973, Soviet Astron.–AJ, 16, 7
Shapiro, P. R., & Sutherland, P. G. 1982, ApJ, 263, 902
Shigeyama, T., Suzuki, T., Kumugai, S., Nomoto, K., Saio, H., & Yamaoka, H. 1994, ApJ, 420, 341
Simmons, J. F. L., & Stewart, B. G. 1985, A&A, 142, 100
Smith, P. 1993, private communication
Sobolev, V. V. 1957, Soviet Astron. J., 1, 297
Spyromilio, J., & Bailey, J. 1993, Proc. Astron. Soc. Australia, 10, 263
Steinmetz, M., & Höflich, P. 1992, A&A, 257, 641
Swartz, D. A., Clocchiatti, A., Benjamin, R., Lester, D. F., & Wheeler, J. C. 1993, Nature, 365, 232
Trammell, S. R., Hines, D. C., & Wheeler, J. C. 1993, ApJ, 414, L21
Tran, H., & Filippenko, A. V. 1993, private communication
Utrobin, V. P. 1995, A&A, in press
Van Dyk, S., Weiler, K. W., Sramek, R. A., Rupen, M. P., & Panagia, N. 1994, ApJ, 432, L115
Wang, L., Li, Z., Clocchiatti, A., Wheeler, J. C., & Wills, D. 1996, in preparation
Wardle, J. F. C., & Kronberg, P. P. 1974 , ApJ, 194, 249
Wheeler, J. C., & Filippenko, A. V. 1995, in Rev. of the Contributions to the Xian Workshop on SN 1993J, ed. D. McCray (Cambridge: Cambridge Univ. Press), in press
Wheeler, J. C., et al. 1993, ApJ, 417, L71
Wheeler J. C., Harkness, R. P., Clocchiatti, A., Benetti, S., Brotherton, M., Depoy, D., & Elias, J. 1994, ApJ, 436, L135
Wilking, B. A., Lebofsky, M. J., & Rieke, G. H. 1982, AJ, 87, 695
Wesselink, A. J. 1946, Bull. Astron. Inst. Netherlands, 368, 91
Wolstencroft, R. D., & Kemp, J. C. 1972, Nature, 238, 45
Woosley, S. E., Eastman, R. G., Weaver, T. A., & Pinto, 1994, ApJ, 429, 300
Yamada, S., & Sato, K. 1991, ApJ, 358, L9